REPORT

Isolated and Syndromic Retinal Dystrophy Caused by Biallelic Mutations in *RCBTB1*, a Gene Implicated in Ubiquitination

Frauke Coppieters,[1,2,18,]* Giulia Ascari,[1,18] Katharina Dannhausen,[3] Konstantinos Nikopoulos,[4] Frank Peelman,[5] Marcus Karlstetter,[3,6] Mingchu Xu,[7] Cécile Brachet,[8] Isabelle Meunier,[9,10,11] Miltiadis K. Tsilimbaris,[12] Chrysanthi Tsika,[12] Styliani V. Blazaki,[12] Sarah Vergult,[1] Pietro Farinelli,[4] Thalia Van Laethem,[1] Miriam Bauwens,[1] Marieke De Bruyne,[1] Rui Chen,[7,13] Thomas Langmann,[3] Ruifang Sui,[14] Françoise Meire,[15] Carlo Rivolta,[4] Christian P. Hamel,[9,10,11] Bart P. Leroy,[1,16,17] and Elfride De Baere[1,]*

Inherited retinal dystrophies (iRDs) are a group of genetically and clinically heterogeneous conditions resulting from mutations in over 250 genes. Here, homozygosity mapping and whole-exome sequencing (WES) in a consanguineous family revealed a homozygous missense mutation, c.973C>T (p.His325Tyr), in *RCBTB1*. In affected individuals, it was found to segregate with retinitis pigmentosa (RP), goiter, primary ovarian insufficiency, and mild intellectual disability. Subsequent analysis of WES data in different cohorts uncovered four additional homozygous missense mutations in five unrelated families in whom iRD segregates with or without syndromic features. Ocular phenotypes ranged from typical RP starting in the second decade to chorioretinal dystrophy with a later age of onset. The five missense mutations affect highly conserved residues either in the sixth repeat of the RCC1 domain or in the BTB1 domain. A founder haplotype was identified for mutation c.919G>A (p.Val307Met), occurring in two families of Mediterranean origin. We showed ubiquitous mRNA expression of *RCBTB1* and demonstrated predominant RCBTB1 localization in human inner retina. RCBTB1 was very recently shown to be involved in ubiquitination, more specifically as a CUL3 substrate adaptor. Therefore, the effect on different components of the CUL3 and NFE2L2 (NRF2) pathway was assessed in affected individuals' lymphocytes, revealing decreased mRNA expression of *NFE2L2* and several NFE2L2 target genes. In conclusion, our study puts forward mutations in *RCBTB1* as a cause of autosomal-recessive non-syndromic and syndromic iRD. Finally, our data support a role for impaired ubiquitination in the pathogenetic mechanism of *RCBTB1* mutations.

Inherited retinal dystrophies (iRDs) are a major cause of blindness worldwide. They compose a group of genetic eye disorders with a broad phenotypic spectrum and variable age of onset and are caused by progressive degeneration of rod and cone photoreceptors and/or the retinal pigment epithelium (RPE).[1] Most iRDs are genetically heterogeneous; mutations have been identified in over 250 genes thus far (RetNet), allowing a molecular diagnosis in up to 80% of cases.[2] Many of these genes were identified on the basis of their role in retina-specific pathways. In recent years, however, an increasing number of defects have been found in ubiquitously expressed genes playing roles not only in retinal pathways but also in more general pathways, e.g., *DHDDS* (dehydrodolichyl diphosphate synthase subunit [MIM: 608172]), *HGSNAT* (heparan-alpha-glucosaminide N-acetyltransferase [MIM: 610453]),

MFSD8 (major facilitator superfamily domain containing 8 [MIM: 611124]), and *MVK* (mevalonate kinase [MIM: 251170]) (RetNet). The isolated retinal phenotypes can often be explained by hypomorphic mutations resulting in partial loss of function, whereas syndromic phenotypes are caused by more severe mutations.[3–5]

The initial aim of this study was to unravel the genetic etiology in a Belgian consanguineous family of Turkish origin (F1) in whom two autosomal-recessive traits segregate in two branches (Figure 1). In the first branch, three females present with retinitis pigmentosa (RP [MIM: 268000], the most common iRD), goiter (MIM: 138800), primary ovarian insufficiency (POI [MIM: 311360]), and mild intellectual disability. In the second branch, two individuals display postaxial polydactyly (MIM: 174200), a feature not present in any of the individuals with RP

[1]Center for Medical Genetics, Ghent University and Ghent University Hospital, 9000 Ghent, Belgium; [2]pxlence BVBA, 9200 Dendermonde, Belgium; [3]Department of Ophthalmology, University of Cologne, 50931 Cologne, Germany; [4]Unit of Medical Genetics, Department of Computational Biology, University of Lausanne, 1011 Lausanne, Switzerland; [5]Flanders Institute for Biotechnology (VIB), Department of Medical Protein Research, Faculty of Medicine and Health Sciences, Ghent University, 9000 Ghent, Belgium; [6]Therapeutic Research Group Ophthalmology, Bayer Pharma AG, 42096 Wuppertal, Germany; [7]Department of Molecular and Human Genetics, Baylor College of Medicine, Houston, TX 77030, USA; [8]Pediatric Endocrinology Unit, Hôpital Universitaire des Enfants Reine Fabiola, Université Libre de Bruxelles, 1000 Brussels, Belgium; [9]Genetic Sensory Diseases, Centre Hospitalier Universitaire de Montpellier, 34295 Montpellier, France; [10]Université Montpellier, 34090 Montpellier, France; [11]INSERM U1051, Institut des Neurosciences de Montpellier, 34091 Montpellier, France; [12]Department of Ophthalmology, Medical School, University of Crete, 71409 Heraklion, Greece; [13]Human Genome Sequencing Center, Baylor College of Medicine, Houston, TX 77030, USA; [14]Department of Ophthalmology, Peking Union Medical College Hospital, Peking Union Medical College, Chinese Academy of Medical Sciences, 100730 Beijing, China; [15]Department of Ophthalmology, Hôpital Universitaire des Enfants Reine Fabiola, 1000 Brussels, Belgium; [16]Department of Ophthalmology, Ghent University Hospital and Ghent University, 9000 Ghent, Belgium; [17]Division of Ophthalmology, The Children's Hospital of Philadelphia, Philadelphia, PA 19104, USA
[18]These authors contributed equally to this work
*Correspondence: frauke.coppieters@ugent.be (F.C.), elfride.debaere@ugent.be (E.D.B.)
http://dx.doi.org/10.1016/j.ajhg.2016.06.017
© 2016 American Society of Human Genetics.

CrossMark

Figure 1. F1 — p.His325Tyr

I:1 I:2 I:3 I:4
II:1 II:2 II:3 II:4 II:5 II:6
III:1 III:2 III:3 III:4 III:5 (M/+) III:6 (M/+) III:7 III:8
WES IBD
IV:1 (M/+) IV:2 (M/+) IV:3 (M/M) IV:4 IV:5 IV:6 IV:7 IV:8 (+/+)
WES IBD
V:1 (M/M) V:2 (M/M) V:3 (M/+) V:4 (M/+) V:5
WES IBD IBD IBD

F2 — p.Val307Met

I:1 I:2
II:1 II:2 II:3 II:4 (M/M) II:5 (M/M) II:6 (M/+) II:7
WES WES WES

F3 — p.Val307Met

I:1 I:2
II:1 (M/M)
WES

F6 — p.Leu388Phe

I:1 II:2
II:1 II:2 (M/M) II:3
WES
III:1 III:2

F4 — p.Trp310Cys

I:1 I:2 I:3 I:4 (M/+)
II:1 II:2 (M/M) II:3 II:4 (M/M) II:5 (M/M) II:6 (M/+) 3
III:1 (M/+) III:2 (M/M)
WES

F5 — M1: p.His384Arg M2: p.Ser401Leu

I:1 I:2
II:1 II:2 II:3 II:4 II:5 II:6 (M1/M1 M2/M2) II:7 II:8
WES
III:1 (M1/+ M2/+)

Legend:
● (isolated) RP
▨ postaxial polydactyly
M mutant allele
+ wild type allele

Figure 1. *RCBTB1* Mutations Identified in Six Families Affected by Syndromic and Non-syndromic iRD
Filled symbols represent affected individuals, whereas clear symbols represent unaffected individuals. A double line represents reported consanguinity. Genotypes of different family members are indicated below them. Individuals who underwent identity-by-descent mapping and/or whole-exome sequencing are indicated by IBD and WES, respectively.

identified in *RCBTB1* (RCC1 and BTB domain containing protein 1 [MIM: 607867]) the homozygous missense variant c.973C>T (p.His325Tyr) (GenBank: NM_018191.3), which is predicted to affect protein function (Figure S1 and Table S1). Segregation of this variant with the disease in the family was confirmed by Sanger sequencing of *RCBTB1* exon 9 (Figure 1). The variant was found to be absent in 142 control individuals, 68 of whom are of Turkish origin. This change is known as rs200826424 in dbSNP and has an overall allele frequency of 0.0091% in the Exome Aggregation Consortium (ExAC) Browser (no homozygotes were observed).

In order to identify additional iRD-affected families with mutations in *RCBTB1*, we performed targeted next-generation sequencing on the coding region of *RCBTB1* as previously described[6] (Table S2) in a Belgian cohort of 281 probands with autosomal-recessive or sporadic iRD. This did not reveal any mutations. Inspection of WES data (Table S3) in ~450 unsolved iRD cases from four cohorts from the European Retinal Disease Consortium revealed homozygous mutations in the probands of five additional families; these individuals display isolated or syndromic iRD with thyroid involvement or sensorineural hearing loss (Table 1).

In all families, the *RCBTB1* mutations are the most likely cause of the common retinal phenotype identified by WES (Table S4). All mutations are missense changes, were identified in a homozygous state in the affected individuals, and segregate with disease in the family (Figure 1). *RCBTB1* is located in the largest (F1 and F4) or third largest (F3) homozygous region in families in whom IBD mapping was performed (Figure S2). As summarized in Table S1, all mutations have very low minor allele frequencies or are absent in the ExAC Browser, and all are predicted to be deleterious. In family F5, two *RCBTB1* variants were identified in *cis*, and both are present in a homozygous state in the

(Figure 1). A summary of the retinal manifestations can be found in Figure 2 and Table 1, and the other clinical features are provided in Table 1 and the Supplemental Note (case report S1). This study was approved by the ethics committee of Ghent University Hospital, adhered to the tenets of the Declaration of Helsinki, and obtained informed consent from all participants. Peripheral blood was collected from affected individuals, parents, and unaffected relatives if available. Genomic DNA was extracted from blood leukocytes according to standard procedures.

Identity-by-descent (IBD) mapping in three affected individuals (IV:3, V:1, and V:2) and one unaffected individual (V:3) revealed a single genomic region (hg38 chr13: 41,246,578–52,963,036) that is homozygous in the affected individuals and heterozygous in the healthy sibling (Affymetrix GeneChip Human Mapping 250K). Subsequent whole-exome sequencing (WES; TruSeq Exome Enrichment, HiSeq 2000, Illumina) in two affected individuals (IV:3 and V:1)
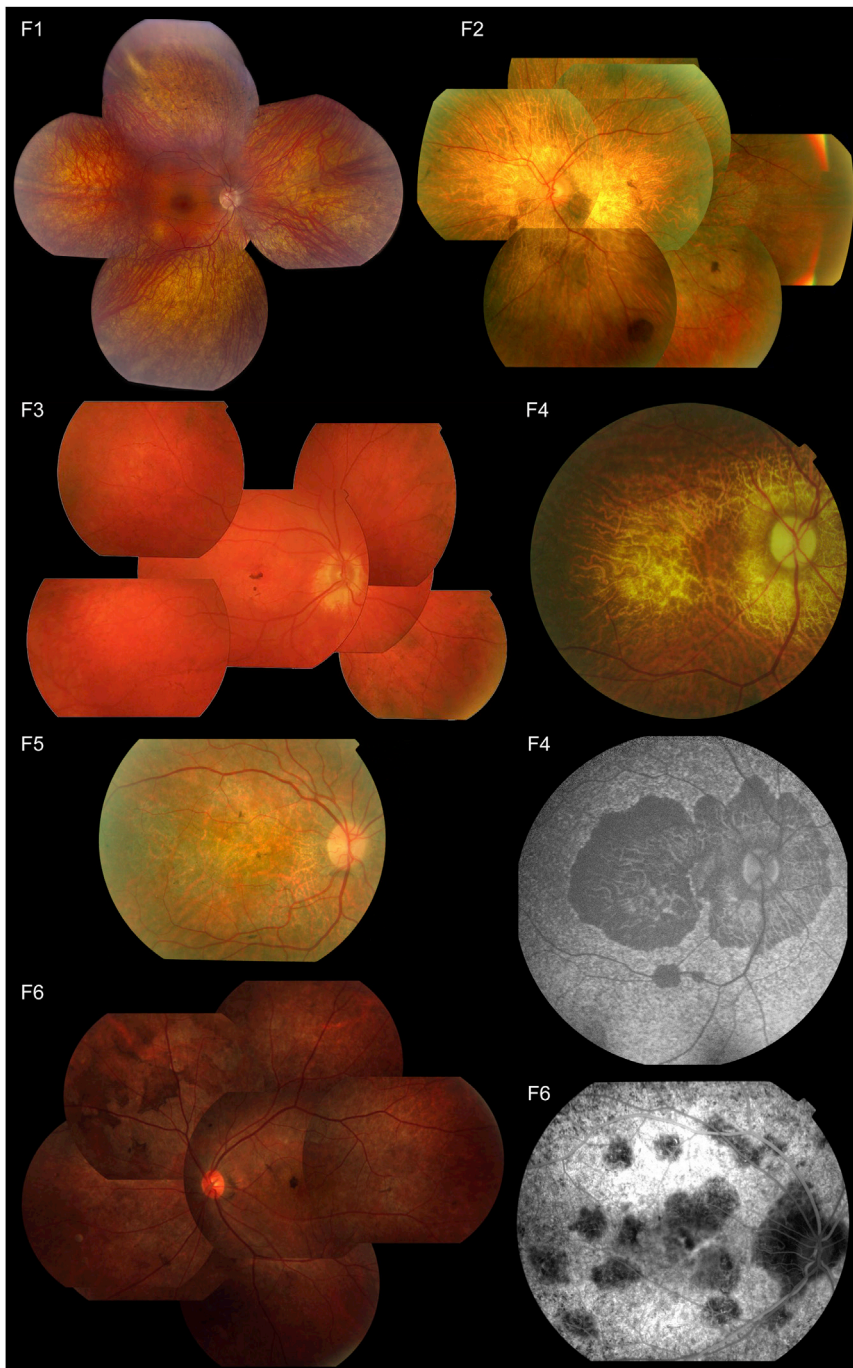
Figure 2. Representative Retinal Pictures of Index Individuals from the Six Families Affected by *RCBTB1*-Associated iRD

(F1) Composite fundus picture of the retinal epithelium of individual V:2 shows outer retinal atrophy, which is more pronounced in the retinal periphery with predominantly spicular intraretinal pigmentation, and a better preserved macula. Overall, this is compatible with a diagnosis of RP.

(F2–F6) Fundus pictures show progressive pattern-like reticular dystrophy in the retinal periphery, fine heterogeneity of pigment epithelium alterations, and rounded spots of chorioretinal macular atrophy (which enlarge with age). (F2) Fundus picture of the left eye of II:4 at age 68 years shows features similar to those of II:2 (F6), i.e., some pigment deposits in the form of large brown spots, as well as retinal atrophy. (F3) Fundus picture of the right eye of II:1 shows central coalescent areas with chorioretinal atrophy and peripheral reticular dystrophy. (F4) Second and third panels, right column: fundus picture and autofluorescence of the right eye of II:5 (67 years) show central and peripapillary chorioretinal atrophy. (F5) Fundus picture of the right eye of II:6 at 55 years. A detailed macular view shows a discolored retina, which reflects the retinal atrophy and a few fine pigment deposits. (F6) Left: fundus picture of LE of II:2 displays features similar to those of II:4 (F2). Right: fluorescence angiography of the right eye of II:2 displays irregular hypofluorescent areas in the posterior pole.

SNPs revealed a 3 Mb common haplotype, which suggests a Mediterranean founder mutation (Figure S3).

RCBTB1 has a regulator of chromosome condensation 1 (RCC1)-like domain (RLD) and two broad complex, tramtrack, and bric-a-brac (BTB) domains (UniProt: Q8NDN9).[7] Three (F1–F4) and two (F5 and F6) of the mutations are located in the sixth repeat of the RLD (RCC6) and in the first BTB domain (BTB1), respectively (Figure 3). The affected and surrounding amino acids are highly conserved throughout evolution (Figure S4).

The BTB domain is a protein-protein-interaction motif with a high degree of sequence variability. Sequence comparison based on structure superposition of different protein families revealed only 15 significantly conserved residues out of 95 amino acids composing the core BTB, and 12 of them are buried in the monomer core. In contrast, highly variable residues are located on the exposed interaction surface and probably contribute to interaction behavior.[15,16] Interestingly, the *RCBTB1*

proband and in a heterozygous state in her unaffected daughter. It is still unclear which of these variants is causal. Both variants have comparable in silico predictions on protein function (Table S1). The c.1151A>G (p.His384Arg) variant affects a highly conserved residue, and protein modeling suggests a disruptive effect, whereas the c.1202C>T (p.Ser401Leu) variant affects a less conserved, surface-exposed residue for which protein modeling is inconclusive (see below).

The c.919G>A (p.Val307Met) mutation was found in two families originating from Italy (F2) and Greece (F3). Segregation analysis with microsatellite markers and

Table 1. Overview of *RCBTB1* Mutations and the Associated Phenotypes Identified in This Study

Family	Origin	Mutation (Zygosity)	Individual	Retinal Phenotype Age of Onset (Years)	Retinal Phenotype Characteristics	Extra-ocular Phenotypic Manifestations
F1	Turkey	c.973C>T (p.His325Tyr) (hom)	V:1	17	severe iRD compatible with RP	goiter, POI, and mild ID
			V:2	14	severe iRD compatible with RP	goiter, POI, mild ID, recurrent otitis media, psoriasis, and allergy to house dust mites
			IV:3	18	severe iRD compatible with RP	goiter, POI, and mild ID
F2	Italy	c.919G>A (p.Val307Met) (hom)	II:4	40	progressive pattern-like reticular dystrophy	none reported
			II:5	55	progressive pattern-like reticular dystrophy	none reported
F3	Greece	c.919G>A (p.Val307Met) (hom)	II:1	50	central chorioretinal atrophy and peripheral reticular dystrophy	thyroid nodules, cold intolerance, and dyslipidemia; son with autism and ID
F4	Greece	c.930G>T (p.Trp310Cys) (hom)	II:5	45	central chorioretinal atrophy and peripheral reticular dystrophy	sensorineural hearing loss (adult onset) and spinal ganglioglioma
			III:2	30	central chorioretinal atrophy and peripheral reticular dystrophy	sensorineural hearing loss (adult onset); mother with reported Hashimoto thyroiditis
F5	Algeria	c.1151A>G (p.His384Arg) (hom) and c.1202C>T (p.Ser401Leu) (hom)	II:6	48	progressive pattern-like reticular dystrophy	lung fibrosis
F6	China	c.1164G>T (p.Leu388Phe) (hom)	II:2	33	retinal dystrophy starting with bilateral vision loss; fundus with bilateral irregular pigmentations mainly in the mid-periphery	none reported

The phenotypes associated with *RCBTB1* mutations vary from a more severe iRD (i.e., RP) and shared extra-ocular features (goiter, POI, and mild ID) in three F1 individuals to progressive iRD with or without extra-ocular features in seven individuals from five families (F2–F6). The clinical onset of iRD in these families is between 30 and 50 years of age, mostly with decreasing visual acuity and an absence of complaints about the peripheral visual field. Fundus pictures show reticular dystrophy in the retinal periphery and rounded spots of chorioretinal macular atrophy, which enlarge with age. Electroretinography is characterized by moderate alterations of all responses (which worsen with age), indicating loss of both rods and cones. Abbreviations are as follows: hom, homozygous; ID, intellectual disability; POI, primary ovarian insufficiency; iRD, inherited retinal dystrophy; and RP, retinitis pigmentosa.

mutations c.1151A>G (p.His384Arg) (F5) and c.1164G>T (p.Leu388Phe) (F6) affect 2 of the 12 highly conserved amino acids. As for the RLD domain, the residues Val307 and Trp310 are both hydrophobic amino acids highly conserved in human RLD superfamily proteins.[17]

We built homology models for both RCBTB1 domains. The models predict a deleterious effect for mutations c.919G>A (p.Val307Met), c.930G>T (p.Trp310Cys), c.1151A>G (p.His384Arg), and c.1164G>T (p.Leu388Phe), whereas the accuracy of the models does not allow predicting the effect of c.973C>T (p.His325Tyr) or c.1202C>T (p.Ser401Leu) (Figure 3).

The retinal phenotype associated with *RCBTB1* mutations varies from a severe iRD compatible with RP to a progressive iRD with central chorioretinal atrophy and peripheral reticular dystrophy (Figure 2 and Table 1). It has previously been described that mutations in a single gene cause distinct iRDs. Well-known examples of genes in which mutations can cause both RP and chorioretinal atrophy are *PRPH2*[18] (peripherin 2 [MIM: 179605]) and *ABCA4*[19] (ATP binding cassette subfamily A member 4 [MIM: 601691]). Possible contributing factors are the nature, severity, and location of the mutated alleles.

Non-ocular features observed in families affected by *RCBTB1* mutations include adult-onset sensorineural hearing loss (F4), lung fibrosis (MIM: 178500; F5), and thyroid involvement (Table 1). The latter was observed in three families. In F1, two sisters have RP, small teeth, goiter with normal thyroid-stimulating hormone (TSH) and free thyroxine (FT4) and the absence of thyroid autoantibodies, higher than normal weight, and mild intellectual disability. In addition, spontaneous pubertal development and menarche at 14 years of age preceded secondary amenorrhea at the age of 15–16 years and gonadotropin elevation, indicating POI. More detailed endocrinological data of individuals V:1 and V:2 are listed in the Supplemental Note (see case report S1). Family history showed a goiter at 38 years of age in the mother (IV:2) and the association of RP, goiter, POI, and slight intellectual disability in a maternal cousin (IV:3). To our knowledge, the association
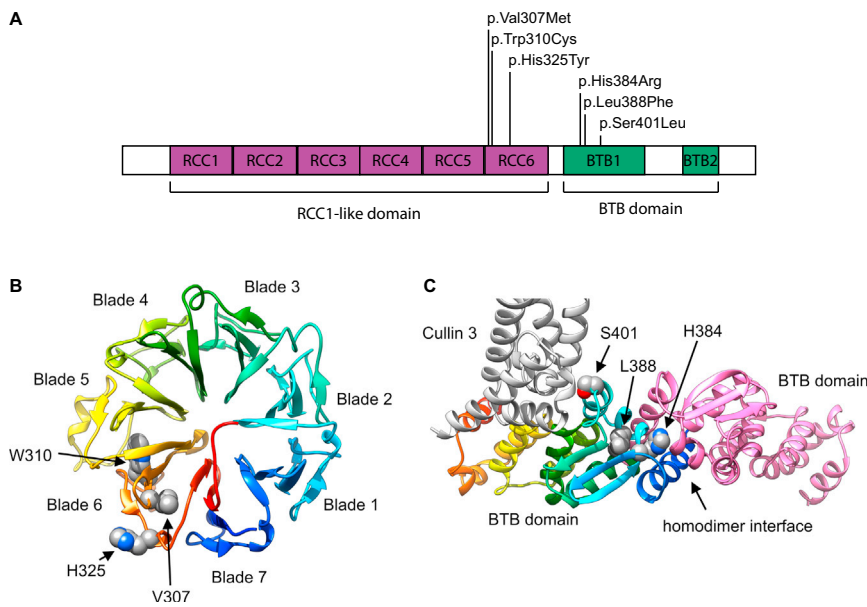
Figure 3. Location and Structural Modeling of Identified RCBTB1 Missense Variants

(A) Schematic diagram of RCBTB1 shows the location of the missense variants within two distinct domains: three (F1–F4) in the sixth repeat of the RCC1-like domain (RLD), i.e., RCC6, and two (F5 and F6) in the first BTB domain (BTB1).

(B) A homology model for the β-propeller structure of the RLD is shown in rainbow colors, evolving from blue (N-terminal) to red (C-terminal). The RCBTB1 RLD contains seven repeats that form a seven-bladed β-propeller, in which each blade consists of a four-stranded antiparallel β sheet. The p.Val307Met (c.919G>A), p.Trp310Cys (c.930G>T), and p.His325Tyr (c.973C>T) variants are all found in the sixth blade. Val307 and Trp310 are part of the third strand of blade 6. Trp310 is a conserved aromatic. The bulky indole group of Trp310 is buried in the hydrophobic core between blades five and six and makes extensive Van der Waals contacts with three aliphatic sidechains of blade five. p.Trp310Cys therefore introduces a big void between both blades and is probably highly destabilizing. Val307 is part of a hydrophobic core between blades six and seven. The more bulky methionine side chain introduced by p.Val307Met is clashing with residues of blade seven. His325 cannot be modeled accurately because alignments with different methods and against different templates give diverging outcomes for the exact position of this residue. Most likely, His325 is surface exposed at the end of the fourth strand of blade six.

(C) A homology model for the RCBTB1 BTB domain is shown in rainbow colors, evolving from blue (N-terminal) to red (C-terminal). Another interacting RCBTB1 BTB domain is shown in pink. Part of an interacting CUL3 molecule is shown in gray. His384 is found at the BTB homodimerization interface. A histidine is present at this position in nine of ten BTB structures aligned with the RCBTB1 BTB domain.[8] His384 forms an extensive hydrogen-bond network at the interfacial area and makes a direct Van der Waals contact with the homodimerization partner. p.His384Arg (c.1151A>G) disrupts the hydrogen-bonding network, and accommodation of two bulky arginine residues in the homodimer interface is impossible. Leu388 is an extremely conserved residue of the hydrophobic BTB core and is identical in all ten crystal structures. p.Leu388Phe (c.1164G>T) introduces drastic steric clashes of the phenyl ring with surrounding hydrophobic residues. Ser401 is a surface-exposed residue that is either close to or at the edge of the BTB-CUL3 interface, depending on the template that was used. It is unclear whether p.Ser401Leu (c.1202C>T) can disrupt the interaction with CUL3. Homology models were built on the basis of different structure templates with YASARA Structure.[9,10] Additional models were built in MODELER and YASARA Structure with alignments based on HHPRED and Phyre2.[8–12] On the basis of the initial models, the alignments were edited for model improvement, as judged by the DOPE score in MODELER, visual inspection, and Verify_3D 3D profile analysis of the models.[11,13] The models are based on template structures of RLD (PDB: 4O2W) and the BTB domain complex (PDB: 4J8Z and 4AP2). The effects of the variants were analyzed in YASARA Structure.[9,10] Figures were generated with UCSF Chimera.[14]

between POI and goiter without auto-immunity has not been described before in a known clinical entity.

For the F3 proband, who suffers from thyroid nodules, cold intolerance, and dyslipidemia, no endocrine data are available. In F4, the mother of the proband (II:6) was diagnosed with Hashimoto thyroiditis (MIM: 140300) on the basis of clinical appearance and laboratory findings. Ultrasound showed a multinodal goiter (increased total thyroid volume with multinodal appearance without neoplastic characteristics). TSH and hormones T3 and T4 were within normal limits, but antibodies against TSH and thyroglobulin were elevated.

Because the combination of iRD and thyroid disease is rare, WES data of F1 were also analyzed for the presence of variants in genes important for thyroid function and/or in which mutations are known to cause thyroid disease, as well as genes located in the shared IBD region and predicted to be related to goiter on the basis of gene-prioritization tools (Table S5 and Figure S5). However, we did not identify variants that could explain the thyroid phenotype (Table S6). Despite this extensive variant analysis, we cannot completely rule out the possibility that mutations in other genes cause the non-ocular phenotypes such as thyroid involvement, especially linked mutations in autozygous regions in the case of consanguineous origin.

So far, little is known about the function of RCBTB1. RCBTB1 was initially identified as a candidate gene for chronic lymphocytic leukemia (MIM: 151400) and was shown to activate the pathway for DNA damage and repair.[7,20,21] In addition, overabundant RCBTB1 induces cellular hypertrophy in cultured rat vascular smooth muscle and renal proximal tubular cells as an angiotensin II type 1 receptor-associated protein, and a synonymous SNP in RCBTB1 modifies the effect of smoking on carotid intima-media thickness.[22,23] In a final stage of this study, haploinsufficiency of RCBTB1 was shown in two families in whom mutations segregate with Coats disease (MIM: 300216) or familial exudative vitreoretinopathy (FEVR [MIM: 133780]). Functional analysis suggested a role for RCBTB1 in retinal angiogenesis through Norrin-induced
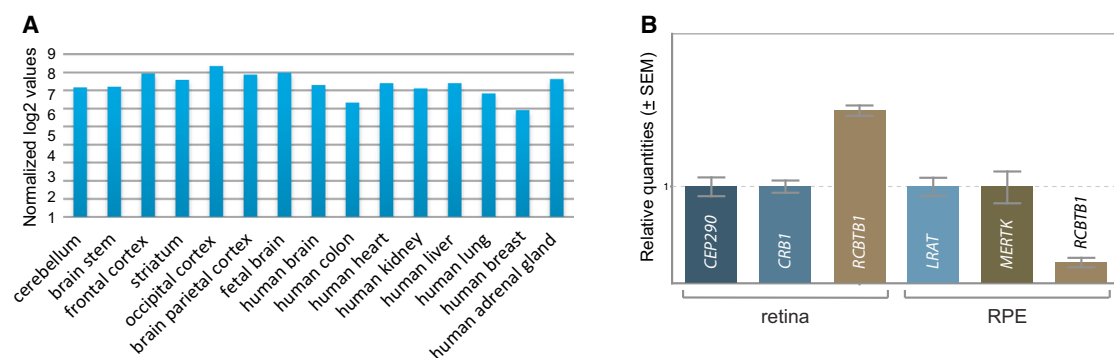
Figure 4. Expression Analysis of *RCBTB1* mRNA

(A) Expression analysis was performed according to the manufacturer's instructions with an in-house-designed custom array (SurePrint G3 Human Gene Expression array version 2, AMADID 041648, Agilent Technologies) covering all protein-coding genes and 22,980 long non-coding RNA transcripts (LNCipedia version 2.1). Data normalization was performed with the VSN package in R. All values were $\log_2$ transformed. Samples included total RNA from whole brain, colon, heart, kidney, liver, lung, breast, and adrenal gland (Stratagene Europe; all adult tissues); cerebellum, brain stem, striatum, frontal cortex, occipital cortex, and parietal cortex (Agilent; adult tissues); and fetal whole brain (Agilent).

(B) qPCR-based expression analysis of mRNA from *RCBTB1* and two positive control genes strongly expressed in the retina and retinal pigment epithelium (RPE) was performed as previously described[25] on commercial human cDNA from retina (BioChain) and RPE (3H Biomedical). High retinal and limited RPE expression was observed. Error bars represent the SE of the relative quantities.

β-catenin signaling. A clinical overlap with RP was excluded in one of the probands given the absence of night blindness, a typical fundus aspect of FEVR without bony spicules or narrow vessels, and a preserved electroretinogram in one eye.[24] In the families included here, no FEVR signs could be observed, sustaining the hypothesis that distinct molecular consequences of *RCBTB1* mutations and zygosity cause different clinical entities.

Because of the syndromic phenotypes observed in this study, we explored the expression pattern of *RCBTB1* human mRNA by analyzing in-house whole-transcriptome expression array data, which showed ubiquitous expression (SurePrint G3 Human Gene Expression array version 2, AMADID 041648, Agilent Technologies) (Figure 4A). Thyroid *RCBTB1* expression was observed in several experiments centralized in the EMBL-EBI Expression Atlas. The gene was found to be moderately expressed in the cochlea, saccule, utricle, and ampulla of the adult human inner ear.[26] Next, we performed targeted analysis of the expression of *RCBTB1* and *Rcbtb1* mRNA in different human and murine tissues, respectively. *RCBTB1* mRNA showed relatively high and limited expression in the human retina and RPE, respectively, and *Rcbtb1* mRNA showed strong expression in the murine retina, RPE, and ovary (Figure 4B and Figure S6). On the basis of these expression results, staining of RCBTB1 was performed on murine and human retinal sections (Figure 5). In the murine retina, RCBTB1 was found mainly in the inner retina with strong signals reaching up to the outer plexiform layer (Figures 5A and 5B). In human sections, immunostaining was present in the nerve fiber layer and to a lesser extent in the inner and outer plexiform layers (Figures 5C and 5D). The staining signal in the photoreceptor layer is very likely due to autofluorescence of outer segments, as described before.[28]

The RCC1-like domain is present in several ciliary proteins, whose encoding genes (*RPGR* [retinitis pigmentosa GTPase regulator (MIM: 312610)], *NEK8* [NIMA related kinase 8 (MIM: 609799)], and recently *NEK9* [NIMA related kinase 9 (MIM: 609798)]) are implicated in Mendelian disease.[29–31] For RPGR and NEK8, this domain is involved in targeting the protein to the photoreceptor connecting cilium and centrosome, respectively.[29,30] Hence, co-staining of RCBTB1 with acetylated α-tubulin was performed in the retina. However, no clear co-staining was observed (Figure S7).

RCBTB1 has previously been shown to be involved in ubiquitination, a post-translational modification with a wide variety of functions, among which is the recognition of proteins for proteasome degradation.[32] In this process, ubiquitin is first activated by an activating enzyme (E1) and then carried by a conjugating enzyme (E2) to a substrate through interaction with a ubiquitin ligase (E3) (Figure S8). RCBTB1 was identified as a putative substrate adaptor for cullin 3 (CUL3). CUL3 is the major component of the CULLIN3-RING ubiquitin ligases (CRL3), an emerging class of E3 enzymes regulating a wide range of cellular and developmental processes (Figure S8).[32,33] Substrate recognition is highly specific and mediated by substrate adaptors such as RCBTB1, which recruit substrates to the CRL3 complex. In addition, RCBTB1 was shown to interact with UBE2E3, an E2 enzyme that is highly present in the retina and is important for modulating the balance between RPE cell proliferation and differentiation.[32,34,35] Recent evidence has shown that UBE2E3 regulates the localization and activity of the stress-response transcription factor NFE2L2 (nuclear factor, erythroid 2 like 2, often called NRF2) in concert with members of the CRL3 complex (Figure S8).[36] The retina is known to be extremely sensitive to oxidative stress. In this way,
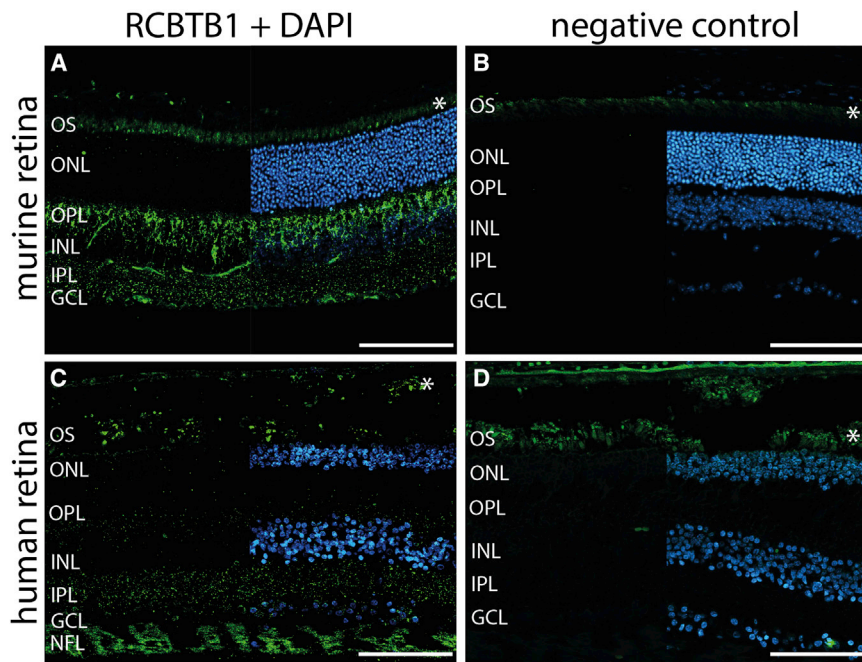
Figure 5. RCBTB1 Staining on Human and Murine Retinal Sections

(A and B) Representative fluorescence images of murine cryosections stained with RCBTB1 antibody (1:100, Abcam) (A) or negative control (B). RCBTB1 immunoreactivity in the murine retina mainly localized to the inner retina.

(C and D) Representative fluorescence images of human paraffin-embedded sections stained with RCBTB1 antibody (1:100, Abcam) (C) or negative control (D). Human RCBTB1 also localized to the inner retina; the strongest signals were detected in the nerve fiber layer. Sections were counterstained with DAPI (blue) and are displayed as split images.

Immunohistochemistry was performed as previously described.[27] Asterisks mark autofluorescence of photoreceptor outer segments. Scale bars represent 100 μm. Abbreviations are as follows: OS, outer segment; IS, inner segment; ONL, outer nuclear layer; OPL, outer plexiform layer; INL, inner nuclear layer; IPL, inner plexiform layer; GCL, ganglion cell layer; and NFL, nerve fiber layer.

NFE2L2 is crucial for protecting and preserving retinal health.[37–40] The stress response mediated by CRL3 and NFE2L2 is also important for other organs, such as the thyroid (affected in families F1, F3, and F4) and the ovaries (affected in family F1). The thyroid in particular requires a stringent regulation of the production and removal of reactive oxygen species in the context of normal hormogenesis and thyroid gland growth.[41,42] Interestingly, a germline loss-of-function mutation in KEAP1 (kelch like ECH associated protein 1 [MIM: 606016]), encoding a CUL3 substrate adaptor that negatively regulates NFE2L2, has been associated with multinodular goiter.[43] In ovarian cells, NFE2L2 is an essential sensor and regulator of chemical homeostasis. NFE2L2-null mice display accelerated ovarian failure after treatment with an ovarian toxicant, and the lack of NFE2L2 results in accelerated ovarian aging.[44,45]

Here, we have demonstrated co-expression of CUL3 (cullin 3 [MIM: 603136]) and RCBTB1 in the human retina and RPE and co-expression of Cul3 and Rcbtb1 in the murine retina, RPE, and ovary (Figure S6). In addition, CUL3 was found in the human retina (faint) and the murine retina, ovary, and thyroid (Figure S9). In order to assess the molecular consequences of RCBTB1 mutations on the CRL3 complex and the NFE2L2 pathway, we analyzed the mRNA expression of CUL3 and RBX1 (ring-box 1 [MIM: 603814]) (encoding two components of the CUL3 complex), UBE2E3 (ubiquitin conjugating enzyme E2 E3 [MIM: 604151]; encoding the protein interacting with RCBTB1), NFE2L2 (nuclear factor, erythroid 2 like 2 [MIM: 600492]), and a selection of 21 NFE2L2 target genes (Table S7).[46,47] Because RCBTB1 is ubiquitously expressed, this analysis was performed on total RNA extracted from peripheral-blood mononuclear cells from two affected individuals from F1 (V:1 and V:2) and six healthy control individuals.

Interestingly, we observed significantly lower expression in affected individuals than in control individuals for CUL3, NFE2L2, and three NFE2L2 target genes: RXRA (retinoid X receptor alpha [MIM: 180245]), IDH1 (isocitrate dehydrogenase [NADP(+)] 1, cytosolic [MIM: 147700]), and SLC25A25 (solute carrier family 25 member 25 [MIM: 608745]) (Figure 6 and Table S8). The decreased expression of CUL3 and NFE2L2 can be explained by autoregulatory feedback loops. NFE2L2 is known to positively regulate the expression of CUL3 in order to control its own degradation.[48] In addition, NFE2L2 is able to autoregulate its own expression.[49] Apart from CUL3 and NFE2L2, some of the NFE2L2 target genes are interesting with respect to the systems affected in the families with RCBTB1 mutations. For example, retinoid X receptor alpha (RXRalpha), encoded by RXRA, is known to be present in the rod inner segment layer, and activation of RXRs prevents photoreceptor oxidative stress-induced apoptosis.[50,51] In addition, RXRs form heterodimers with thyroid hormone receptor and can coregulate response elements.[52] IDH1 is highly expressed in the retina,[53] and IDH1 mutations occur in thyroid cancer.[54] The downregulation of only a limited number of the selected NFE2L2 target genes could be related to the source of the material and/or the absence of oxidative stress at the moment of RNA extraction.

In addition to regulating NFE2L2, RCBTB1 might exert other functions as well. Ubiquitination plays an important role in retinal development, modulation of the visual cycle, and removal of aberrant or misfolded proteins.[55] Pathological accumulation and aggregation of proteins escaping or saturating proteasome degradation is a known iRD disease mechanism.[56,57] This hypothesis requires further studies, however, because RCBTB1 substrates are yet to be identified.
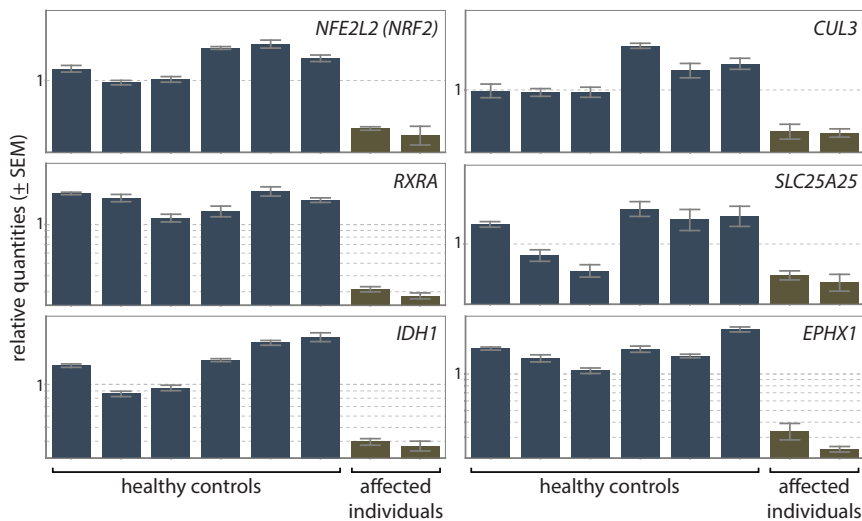
Figure 6. Expression Analysis of *NFE2L2*, *CUL3*, and Four NRF2 Target Genes

The expression of *NFE2L2*, *CUL3*, *RXRA*, *SLC25A25*, and *IDH1* was significantly lower in two affected individuals (V:1 and V:2 from F1) than in six healthy control individuals (respective p values are 0.001, 0.005, 0.001, 0.026, and 0.002). For *EPHX1*, the observed decrease was not significant (p value of 0.076). qPCR expression analysis was performed as previously described.[25] Error bars represent the SE of the relative quantities.

So far, only a few genes in which mutations cause iRD are known to play a role in ubiquitination. Mutations in *KLHL7* (kelch like family member 7 [MIM: 611119]), encoding a CUL3 substrate adaptor, cause autosomal-dominant RP by attenuating ubiquitin ligase activity.[58,59] A second example is *TOPORS* (TOP1 binding arginine/serine rich protein [MIM: 609507]), mutations in which underlie autosomal-dominant RP as well. TOPORS was initially characterized as both a ubiquitin and a SUMO-1 E3 ligase.[60,61] Interestingly, TOPORS is also a cilia-centrosomal protein implicated in ciliary protein trafficking.[62] This is in line with recent studies linking several ubiquitination components with ciliogenesis.[63,64] Mutations in ubiquitously expressed genes with a role in ciliary, lysosomal, or metabolic pathways, for instance, are increasingly described in both isolated and syndromic iRD (RetNet). Mutations in such genes cover a broad spectrum ranging from hypomorphic to null alleles. Depending on the combination of alleles, phenotypes can vary from mild (isolated iRD) to severe (syndromic iRD). In the case of RCBTB1, we hypothesize that the identified missense mutations affect specific functions of the protein and/or distinct protein-protein interactions and thereby impair one or multiple organ systems.

Understanding the pathogenetic mechanism of iRD mutations in genes acting in ubiquitination and downstream NFE2L2 regulation is important in view of therapeutic developments. Local AAV-mediated overexpression of *NFE2L2* was recently put forward as a strategy for prolonging cone survival in three RP models caused by mutations in two different genes (*Pde6b* and *Rho*).[65] In many iRDs, cone loss is secondary to rod degeneration and might be, at least in part, correlated with oxidative stress resulting from massive rod death. Generic, antioxidant gene therapies such as *NFE2L2* overexpression would be much cheaper and easier to implement than gene-specific augmentation therapies.[66]

In conclusion, we have identified *RCBTB1* mutations as a cause of autosomal-recessive iRD with or without extra-

ocular manifestations in the thyroid, ovary, and inner ear. This study has linked autosomal-recessive iRD with impaired ubiquitination and NFE2L2 regulation, an emerging pathway that regulates oxidative stress in the retina and is amenable to gene therapy.

Accession Numbers

The accession numbers for the variants reported in this article are ClinVar: SCV000292417, SCV000292418, SCV000292419, SCV000292420, SCV000292421, and SCV000292422.

Supplemental Data

Supplemental Data include a Supplemental Note, nine figures, and eight tables and can be found with this article online at http://dx.doi.org/10.1016/j.ajhg.2016.06.017.

Conflicts of Interest

F.C. is a co-founder of pxlence.

Acknowledgments

Web Resources

ClinVar, http://www.ncbi.nlm.nih.gov/clinvar
EMBL-EBI Expression Atlas, https://www.ebi.ac.uk/gxa
European Retinal Disease Consortium (ERDC), http://www.erdc.info
OMIM, http://www.omim.org
pxlence, https://www.pxlence.com
RefSeq, http://www.ncbi.nlm.nih.gov/RefSeq
RetNet, https://sph.uth.edu/retnet
UniProt, http://www.uniprot.org
Verify_3D, http://services.mbi.ucla.edu/Verify_3D

References

1. Berger, W., Kloeckener-Gruissem, B., and Neidhardt, J. (2010). The molecular basis of human retinal and vitreoretinal diseases. Prog. Retin. Eye Res. *29*, 335–375.

2. Lee, K., and Garg, S. (2015). Navigating the current landscape of clinical genetic testing for inherited retinal dystrophies. Genet. Med. *17*, 245–252.

3. Lenassi, E., Vincent, A., Li, Z., Saihan, Z., Coffey, A.J., Steele-Stallard, H.B., Moore, A.T., Steel, K.P., Luxon, L.M., Héon, E., et al. (2015). A detailed clinical and molecular survey of subjects with nonsyndromic USH2A retinopathy reveals an allelic hierarchy of disease-causing variants. Eur. J. Hum. Genet. *23*, 1318–1327.

4. Roosing, S., van den Born, L.I., Sangermano, R., Banfi, S., Koenekoop, R.K., Zonneveld-Vrieling, M.N., Klaver, C.C., van Lith-Verhoeven, J.J., Cremers, F.P., den Hollander, A.I., and Hoyng, C.B. (2015). Mutations in MFSD8, encoding a lysosomal membrane protein, are associated with nonsyndromic autosomal recessive macular dystrophy. Ophthalmology *122*, 170–179.

5. Xu, M., Yamada, T., Sun, Z., Eblimit, A., Lopez, I., Wang, F., Manya, H., Xu, S., Zhao, L., Li, Y., et al. (2016). Mutations in POMGNT1 cause non-syndromic retinitis pigmentosa. Hum. Mol. Genet. *25*, 1479–1488.

6. De Leeneer, K., Hellemans, J., Steyaert, W., Lefever, S., Vereecke, I., Debals, E., Crombez, B., Baetens, M., Van Heetvelde, M., Coppieters, F., et al. (2015). Flexible, scalable, and efficient targeted resequencing on a benchtop sequencer for variant detection in clinical practice. Hum. Mutat. *36*, 379–387.

7. Mabuchi, H., Fujii, H., Calin, G., Alder, H., Negrini, M., Rassenti, L., Kipps, T.J., Bullrich, F., and Croce, C.M. (2001). Cloning and characterization of CLLD6, CLLD7, and CLLD8, novel candidate genes for leukemogenesis at chromosome 13q14, a region commonly deleted in B-cell chronic lymphocytic leukemia. Cancer Res. *61*, 2870–2877.

8. Söding, J., Biegert, A., and Lupas, A.N. (2005). The HHpred interactive server for protein homology detection and structure prediction. Nucleic Acids Res. *33*, W244–W248.

9. Krieger, E., Joo, K., Lee, J., Lee, J., Raman, S., Thompson, J., Tyka, M., Baker, D., and Karplus, K. (2009). Improving physical realism, stereochemistry, and side-chain accuracy in homology modeling: Four approaches that performed well in CASP8. Proteins *77 (Suppl 9)*, 114–122.

10. Krieger, E., and Vriend, G. (2015). New ways to boost molecular dynamics simulations. J. Comput. Chem. *36*, 996–1007.

11. Webb, B., and Sali, A. (2014). Comparative Protein Structure Modeling Using MODELLER. Curr. Protoc. Bioinformatics *47*, 1–32.

12. Kelley, L.A., Mezulis, S., Yates, C.M., Wass, M.N., and Sternberg, M.J. (2015). The Phyre2 web portal for protein modeling, prediction and analysis. Nat. Protoc. *10*, 845–858.

13. Bowie, J.U., Lüthy, R., and Eisenberg, D. (1991). A method to identify protein sequences that fold into a known three-dimensional structure. Science *253*, 164–170.

14. Pettersen, E.F., Goddard, T.D., Huang, C.C., Couch, G.S., Greenblatt, D.M., Meng, E.C., and Ferrin, T.E. (2004). UCSF Chimera–a visualization system for exploratory research and analysis. J. Comput. Chem. *25*, 1605–1612.

15. Perez-Torrado, R., Yamada, D., and Defossez, P.A. (2006). Born to bind: the BTB protein-protein interaction domain. BioEssays *28*, 1194–1202.

16. Stogios, P.J., Downs, G.S., Jauhal, J.J., Nandra, S.K., and Privé, G.G. (2005). Sequence and structural analysis of BTB domain proteins. Genome Biol. *6*, R82.

17. Hadjebi, O., Casas-Terradellas, E., Garcia-Gonzalo, F.R., and Rosa, J.L. (2008). The RCC1 superfamily: from genes, to function, to disease. Biochim. Biophys. Acta *1783*, 1467–1479.

18. Renner, A.B., Fiebig, B.S., Weber, B.H., Wissinger, B., Andreasson, S., Gal, A., Cropp, E., Kohl, S., and Kellner, U. (2009). Phenotypic variability and long-term follow-up of patients with known and novel PRPH2/RDS gene mutations. Am. J. Ophthalmol. *147*, 518–530.e1.

19. Burke, T.R., and Tsang, S.H. (2011). Allelic and phenotypic heterogeneity in ABCA4 mutations. Ophthalmic Genet. *32*, 165–174.

20. Solomou, E.E., Sfikakis, P.P., Kotsi, P., Papaioannou, M., Karali, V., Vervessou, E., Hoffbrand, A.V., and Panayiotidis, P. (2003). 13q deletion in chronic lymphocytic leukemia: characterization of E4.5, a novel chromosome condensation regulator-like guanine nucleotide exchange factor. Leuk. Lymphoma *44*, 1579–1585.

21. Zhou, X., and Münger, K. (2010). Clld7, a candidate tumor suppressor on chromosome 13q14, regulates pathways of DNA damage/repair and apoptosis. Cancer Res. *70*, 9434–9443.

22. Guo, D.F., Tardif, V., Ghelima, K., Chan, J.S., Ingelfinger, J.R., Chen, X., and Chenier, I. (2004). A novel angiotensin II type 1 receptor-associated protein induces cellular hypertrophy in rat vascular smooth muscle and renal proximal tubular cells. J. Biol. Chem. *279*, 21109–21120.

23. Wang, L., Rundek, T., Beecham, A., Hudson, B., Blanton, S.H., Zhao, H., Sacco, R.L., and Dong, C. (2014). Genome-wide interaction study identifies RCBTB1 as a modifier for smoking effect on carotid intima-media thickness. Arterioscler. Thromb. Vasc. Biol. *34*, 219–225.

24. Wu, J.H., Liu, J.H., Ko, Y.C., Wang, C.T., Chung, Y.C., Chu, K.C., Liu, T.T., Chao, H.M., Jiang, Y.J., Chen, S.J., and Chung, M.Y. (2016). Haploinsufficiency of RCBTB1 is associated with Coats disease and familial exudative vitreoretinopathy. Hum. Mol. Genet. *25*, 1637–1647.

25. Derveaux, S., Vandesompele, J., and Hellemans, J. (2010). How to do successful gene expression analysis using real-time PCR. Methods *50*, 227–230.

26. Schrauwen, I., Hasin-Brumshtein, Y., Corneveaux, J.J., Ohmen, J., White, C., Allen, A.N., Lusis, A.J., Van Camp, G., Huentelman, M.J., and Friedman, R.A. (2016). A comprehensive

catalogue of the coding and non-coding transcripts of the human inner ear. Hear. Res. *333*, 266–274.

27. Karlstetter, M., Sorusch, N., Caramoy, A., Dannhausen, K., Aslanidis, A., Fauser, S., Boesl, M.R., Nagel-Wolfrum, K., Tamm, E.R., Jägle, H., et al. (2014). Disruption of the retinitis pigmentosa 28 gene Fam161a in mice affects photoreceptor ciliary structure and leads to progressive retinal degeneration. Hum. Mol. Genet. *23*, 5197–5210.

28. Petty, H.R., Elner, V.M., Kawaji, T., Clark, A., Thompson, D., and Yang, D.L. (2010). A facile method for immunofluorescence microscopy of highly autofluorescent human retinal sections using nanoparticles with large Stokes shifts. J. Neurosci. Methods *191*, 222–226.

29. Zhao, Y., Hong, D.H., Pawlyk, B., Yue, G., Adamian, M., Grynberg, M., Godzik, A., and Li, T. (2003). The retinitis pigmentosa GTPase regulator (RPGR)- interacting protein: subserving RPGR function and participating in disk morphogenesis. Proc. Natl. Acad. Sci. USA *100*, 3965–3970.

30. Zalli, D., Bayliss, R., and Fry, A.M. (2012). The Nek8 protein kinase, mutated in the human cystic kidney disease nephronophthisis, is both activated and degraded during ciliogenesis. Hum. Mol. Genet. *21*, 1155–1171.

31. Casey, J.P., Brennan, K., Scheidel, N., McGettigan, P., Lavin, P.T., Carter, S., Ennis, S., Dorkins, H., Ghali, N., Blacque, O.E., et al. (2016). Recessive NEK9 mutation causes a lethal skeletal dysplasia with evidence of cell cycle and ciliary defects. Hum. Mol. Genet. *25*, 1824–1835.

32. Plafker, K.S., Singer, J.D., and Plafker, S.M. (2009). The ubiquitin conjugating enzyme, UbcM2, engages in novel interactions with components of cullin-3 based E3 ligases. Biochemistry *48*, 3527–3537.

33. Genschik, P., Sumara, I., and Lechner, E. (2013). The emerging family of CULLIN3-RING ubiquitin ligases (CRL3s): cellular functions and disease implications. EMBO J. *32*, 2307–2320.

34. Mirza, S., Plafker, K.S., Aston, C., and Plafker, S.M. (2010). Expression and distribution of the class III ubiquitin-conjugating enzymes in the retina. Mol. Vis. *16*, 2425–2437.

35. Plafker, K.S., Farjo, K.M., Wiechmann, A.F., and Plafker, S.M. (2008). The human ubiquitin conjugating enzyme, UBE2E3, is required for proliferation of retinal pigment epithelial cells. Invest. Ophthalmol. Vis. Sci. *49*, 5611–5618.

36. Plafker, K.S., and Plafker, S.M. (2015). The ubiquitin-conjugating enzyme UBE2E3 and its import receptor importin-11 regulate the localization and activity of the antioxidant transcription factor NRF2. Mol. Biol. Cell *26*, 327–338.

37. Zhong, Q., Mishra, M., and Kowluru, R.A. (2013). Transcription factor Nrf2-mediated antioxidant defense system in the development of diabetic retinopathy. Invest. Ophthalmol. Vis. Sci. *54*, 3941–3948.

38. Himori, N., Yamamoto, K., Maruyama, K., Ryu, M., Taguchi, K., Yamamoto, M., and Nakazawa, T. (2013). Critical role of Nrf2 in oxidative stress-induced retinal ganglion cell death. J. Neurochem. *127*, 669–680.

39. Sachdeva, M.M., Cano, M., and Handa, J.T. (2014). Nrf2 signaling is impaired in the aging RPE given an oxidative insult. Exp. Eye Res. *119*, 111–114.

40. Zhao, Z., Chen, Y., Wang, J., Sternberg, P., Freeman, M.L., Grossniklaus, H.E., and Cai, J. (2011). Age-related retinopathy in NRF2-deficient mice. PLoS ONE *6*, e19456.

41. Poncin, S., Colin, I.M., and Gérard, A.C. (2009). Minimal oxidative load: a prerequisite for thyroid cell function. J. Endocrinol. *201*, 161–167.

42. Poncin, S., Van Eeckoudt, S., Humblet, K., Colin, I.M., and Gérard, A.C. (2010). Oxidative stress: a required condition for thyroid cell proliferation. Am. J. Pathol. *176*, 1355–1363.

43. Teshiba, R., Tajiri, T., Sumitomo, K., Masumoto, K., Taguchi, T., and Yamamoto, K. (2013). Identification of a KEAP1 germline mutation in a family with multinodular goitre. PLoS ONE *8*, e65141.

44. Hu, X., Roberts, J.R., Apopa, P.L., Kan, Y.W., and Ma, Q. (2006). Accelerated ovarian failure induced by 4-vinyl cyclohexene diepoxide in Nrf2 null mice. Mol. Cell. Biol. *26*, 940–954.

45. Lim, J., Ortiz, L., Nakamura, B.N., Hoang, Y.D., Banuelos, J., Flores, V.N., Chan, J.Y., and Luderer, U. (2015). Effects of deletion of the transcription factor Nrf2 and benzo [a]pyrene treatment on ovarian follicles and ovarian surface epithelial cells in mice. Reprod. Toxicol. *58*, 24–32.

46. Suzuki, T., Motohashi, H., and Yamamoto, M. (2013). Toward clinical application of the Keap1-Nrf2 pathway. Trends Pharmacol. Sci. *34*, 340–346.

47. Al-Sawaf, O., Clarner, T., Fragoulis, A., Kan, Y.W., Pufe, T., Streetz, K., and Wruck, C.J. (2015). Nrf2 in health and disease: current and future clinical implications. Clin. Sci. *129*, 989–999.

48. Kaspar, J.W., and Jaiswal, A.K. (2010). An autoregulatory loop between Nrf2 and Cul3-Rbx1 controls their cellular abundance. J. Biol. Chem. *285*, 21349–21358.

49. Kwak, M.K., Itoh, K., Yamamoto, M., and Kensler, T.W. (2002). Enhanced expression of the transcription factor Nrf2 by cancer chemopreventive agents: role of antioxidant response element-like sequences in the nrf2 promoter. Mol. Cell. Biol. *22*, 2883–2892.

50. Janssen, J.J., Kuhlmann, E.D., van Vugt, A.H., Winkens, H.J., Janssen, B.P., Deutman, A.F., and Driessen, C.A. (1999). Retinoic acid receptors and retinoid X receptors in the mature retina: subtype determination and cellular distribution. Curr. Eye Res. *19*, 338–347.

51. German, O.L., Monaco, S., Agnolazza, D.L., Rotstein, N.P., and Politi, L.E. (2013). Retinoid X receptor activation is essential for docosahexaenoic acid protection of retina photoreceptors. J. Lipid Res. *54*, 2236–2246.

52. Hsu, J.H., Zavacki, A.M., Harney, J.W., and Brent, G.A. (1995). Retinoid-X receptor (RXR) differentially augments thyroid hormone response in cell lines as a function of the response element and endogenous RXR content. Endocrinology *136*, 421–430.

53. Aijaz, S., Allen, J., Tregidgo, R., van Heyningen, V., Hanson, I., and Clark, B.J. (2005). Expression analysis of SIX3 and SIX6 in human tissues reveals differences in expression and a novel correlation between the expression of SIX3 and the genes encoding isocitrate dehyhrogenase and cadherin 18. Genomics *86*, 86–99.

54. Murugan, A.K., Bojdani, E., and Xing, M. (2010). Identification and functional characterization of isocitrate dehydrogenase 1 (IDH1) mutations in thyroid cancer. Biochem. Biophys. Res. Commun. *393*, 555–559.

55. Campello, L., Esteve-Rudd, J., Cuenca, N., and Martín-Nieto, J. (2013). The ubiquitin-proteasome system in retinal health and disease. Mol. Neurobiol. *47*, 790–810.

56. Illing, M.E., Rajan, R.S., Bence, N.F., and Kopito, R.R. (2002). A rhodopsin mutant linked to autosomal dominant retinitis pigmentosa is prone to aggregate and interacts with the

ubiquitin proteasome system. J. Biol. Chem. *277*, 34150–34160.

57. Vasireddy, V., Jablonski, M.M., Khan, N.W., Wang, X.F., Sahu, P., Sparrow, J.R., and Ayyagari, R. (2009). Elovl4 5-bp deletion knock-in mouse model for Stargardt-like macular degeneration demonstrates accumulation of ELOVL4 and lipofuscin. Exp. Eye Res. *89*, 905–912.

58. Friedman, J.S., Ray, J.W., Waseem, N., Johnson, K., Brooks, M.J., Hugosson, T., Breuer, D., Branham, K.E., Krauth, D.S., Bowne, S.J., et al. (2009). Mutations in a BTB-Kelch protein, KLHL7, cause autosomal-dominant retinitis pigmentosa. Am. J. Hum. Genet. *84*, 792–800.

59. Kigoshi, Y., Tsuruta, F., and Chiba, T. (2011). Ubiquitin ligase activity of Cul3-KLHL7 protein is attenuated by autosomal dominant retinitis pigmentosa causative mutation. J. Biol. Chem. *286*, 33613–33621.

60. Rajendra, R., Malegaonkar, D., Pungaliya, P., Marshall, H., Rasheed, Z., Brownell, J., Liu, L.F., Lutzker, S., Saleem, A., and Rubin, E.H. (2004). Topors functions as an E3 ubiquitin ligase with specific E2 enzymes and ubiquitinates p53. J. Biol. Chem. *279*, 36440–36444.

61. Weger, S., Hammer, E., and Heilbronn, R. (2005). Topors acts as a SUMO-1 E3 ligase for p53 in vitro and in vivo. FEBS Lett. *579*, 5007–5012.

62. Chakarova, C.F., Khanna, H., Shah, A.Z., Patil, S.B., Sedmak, T., Murga-Zamalloa, C.A., Papaioannou, M.G., Nagel-Wolfrum, K., Lopez, I., Munro, P., et al. (2011). TOPORS, implicated in retinal degeneration, is a cilia-centrosomal protein. Hum. Mol. Genet. *20*, 975–987.

63. Kasahara, K., Kawakami, Y., Kiyono, T., Yonemura, S., Kawamura, Y., Era, S., Matsuzaki, F., Goshima, N., and Inagaki, M. (2014). Ubiquitin-proteasome system controls ciliogenesis at the initial step of axoneme extension. Nat. Commun. *5*, 5081.

64. Wheway, G., Schmidts, M., Mans, D.A., Szymanska, K., Nguyen, T.M., Racher, H., Phelps, I.G., Toedt, G., Kennedy, J., Wunderlich, K.A., et al.; UK10K Consortium; University of Washington Center for Mendelian Genomics (2015). An siRNA-based functional genomics screen for the identification of regulators of ciliogenesis and ciliopathy genes. Nat. Cell Biol. *17*, 1074–1087.

65. Xiong, W., MacColl Garfinkel, A.E., Li, Y., Benowitz, L.I., and Cepko, C.L. (2015). NRF2 promotes neuronal survival in neurodegeneration and acute nerve damage. J. Clin. Invest. *125*, 1433–1445.

66. Ramachandran, P.S., Song, J.Y., and Bennett, J. (2015). Exploiting metabolic and antioxidant pathways to maintain vision in blinding disease. J. Clin. Invest. *125*, 1390–1392.